Expression of Functionality of α-Chymotrypsin. The Structure of a Fluorescent Probe–α-Chymotrypsin Complex and the Nature of Its pH Dependence†

Lawrence D. Weber,‡ A. Tulinsky,* J. David Johnson,§ and M. Ashraf El-Bayoumi

ABSTRACT: The 2.8-Å resolution X-ray crystallographic structure of the complex between the fluorescent probe 1-anilinonaphthalene-8-sulfonate (Ans) and α-chymotrypsin (α-CHT) has been determined at pH 3.6 and 6.6. At pH 3.6, Ans binds at a single site on the surface of the enzyme close to the amino terminus of the A chain and interacts intimately with the disulfide bond of Cys-1–122 to produce a highly fluorescent Ans–α-CHT complex. The Ans is bound to α-CHT such that it appears to be exposed to ordered solvent from one side and polar residues from the other. The fluorescence enhancement at low pH does not therefore reflect a hydrophobic site but rather one where the local dipoles do not relax substantially during the excited-state lifetime of Ans. The binding of Ans to α-CHT in crystals does not produce any major changes in the structure of the enzyme. From the similarity of the fluorescence lifetime of Ans in solutions and crystals of α-CHT and fluorescence quenching studies using PtI_4^{2-} the Ans binding site has been shown to be the same in the crystal as in solution. When the pH of Ans–α-CHT crystals is raised to 6.6, the Ans and its protein environment remain essentially the same. The only structural changes occurring with change in pH are those attendant to the formation of the pH 5.4 conformer. The fluorescence decay of Ans–α-CHT crystals remains essentially the same as the pH is changed from 3.6 to 6.6. The fluorescence dependence observed with pH in solution may be due to an increase in the degree of mobility of the water molecules surrounding the Ans as the pH is increased. All of these results show that fluorescence enhancements that occur upon the binding of fluorescent probes to proteins may not always result from a hydrophobic site on the protein and suggest the need for caution in the interpretations of fluorescent changes as such probes interact with macromolecules.

The fluorescent probe 1-anilinonaphthalene-8-sulfonate (Ans) has been used extensively to study the structure of both proteins and membranes and used to monitor structural changes in each (Edelman & McClure, 1968; Brand & Gohlke, 1972). The fluorophore displays characteristic intense high-energy fluorescence in nonpolar or viscous solvents while the fluorescence is essentially weak and of low energy in polar, nonviscous solvents. Many studies have implicated a variety of mechanisms such as the existence of two fluorescent states, one of which is an intramolecular charge-transfer state (Kosower et al., 1975), different emission properties of different Ans conformations (Penzer, 1972), and a "universal" solvent-excited solute interaction (DeToma et al., 1976). In all of these, a means is provided whereby the solvent may increase the nonradiative processes and/or decrease radiative ones and thereby quench Ans fluorescence.

In general, it appears that, in the absence of a chemical quenching group, the quenching of Ans fluorescence is dependent upon the ability of polar molecules to relax during the lifetime of its excited state. Therefore, in a nonpolar environment, such as a hydrophobic region of a protein or within a lipid bilayer, Ans would be expected to fluoresce intensely at high energy. It is also possible, however, for Ans to be bound in a polar region of a macromolecule. If the polar groups are relatively immobile and are unable to relax during the excited-state lifetime of Ans, an intense fluorescence would be expected.

X-ray crystallographic methods have been used to study the binding of salicylate derivatives to liver alcohol dehydrogenase (Einarsson et al., 1974), where it was shown that the salicylate binds in the hydrophobic adenosine-binding pocket. Moreover, the accompanying solution fluorescence studies showed that Ans competes with salicylate derivatives for this binding site. However, no crystallographic studies of the Ans binding were reported. Thus, in order to understand more fully the binding of Ans to proteins, the fluorescence enhancement upon binding, and the mechanism of fluorescence change induced with pH or other protein conformational changes, we have mapped the protein molecular environment of Ans X-ray crystallographically in crystals of α-chymotrypsin (α-CHT) at two different pH values (pH 3.6 and 6.6). In addition, we have performed a number of different fluorescence measurements of Ans in crystals and solutions of α-CHT under various conditions.

Experimental Section

Ans–α-CHT at pH 3.6. Single crystals of α-CHT stored under a 75% saturated solution of ammonium sulfate at pH 3.6 were soaked with a solution of identical composition but saturated with Ans. Standing for several days, the crystals became highly fluorescent. The emission spectrum of Ans–α-CHT in a solution at pH 3.6 has been compared with that observed from crystals, and both show an emission maximum near 484 nm (Johnson, 1978). The striking similarity between the two suggests that the local molecular environment of Ans in the crystal is the same as that in solution.

A more sensitive property to compare in this regard is the quantum yield of the Ans fluorescence, but an accurate direct experimental determination of this quantity is not feasible with the protein crystals. However, a related property is fluorescence lifetime which can be accurately measured by the use of single-photon-counting techniques. The fluorescence

† From the Departments of Chemistry (L.D.W., A.T., and M.A.E.-B.) and Biophysics (J.D.J. and M.A.E.-B.), Michigan State University, East Lansing, Michigan 48824. *Received October 17, 1978; revised manuscript received January 3, 1979.* This work was supported by National Institutes of Health Grants GM 21225-01, GM 21225-02, and GM 21225-03 and in part by funds from National Institutes of Health Training Grant GM-01422 and the College of Osteopathic Medicine and the College of Human Medicine of Michigan State University. For the preceding communication of this series see Hibbard & Tulinsky (1978).

‡ Present address: Biology Department, Massachusetts Institute of Technology, Cambridge, MA 02139.

§ Present address: Department of Pharmacology and Cell Biophysics, University of Cincinnati School of Medicine, Cincinnati, OH 45267.

0006-2960/79/0418-1297$01.00/0

Table I: Unit Cell Parameters of Native and Ans-α-CHT pH Conformers

	a (Å)	b (Å)	c (Å)	β (deg)	$V \times 10^3$(Å^3)
native, pH 3.6	49.24 (7)	67.20 (10)	65.94 (9)	101.76 (6)	213.60 (10)
Ans-α-CHT, pH 3.6	49.32 (4)	67.38 (4)	66.02 (6)	101.80 (4)	214.80 (5)
Ans-α-CHT, pH 3.6[a]	49.52 (5)	67.55 (6)	66.04 (7)	101.88 (4)	216.20 (6)
Ans-α-CHT, pH 6.6	49.24 (5)	67.31 (6)	65.62 (7)	102.07 (6)	212.70 (7)
native, pH 5.4	49.13 (5)	67.83 (7)	65.81 (7)	101.92 (6)	214.60 (7)

[a] Six-month soak.

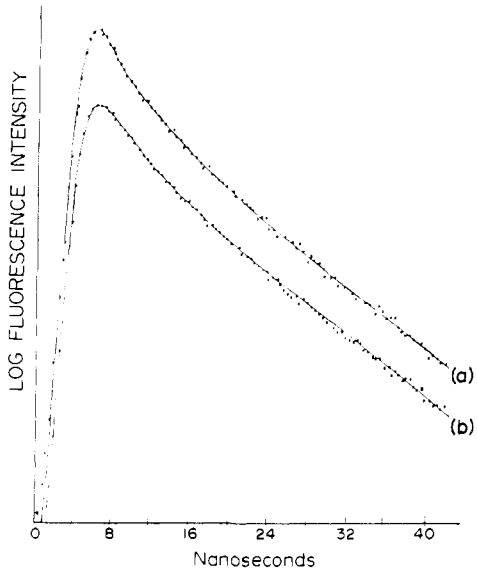

FIGURE 1: Fluorescence decay curves of α-CHT (10^{-4} M) plus Ans (5.2×10^{-5} M) in 0.067 M acetate buffer at pH 3.6 (a) and Ans-α-CHT, pH 3.6, crystals (b). In each case, Ans emission was monitored at 490 nm.

decay curves of Ans-α-CHT in solution and in the crystal at pH 3.6 are shown in Figure 1. A least-squares analysis of the decay curves gives a lifetime of 11.9 ns for both the solution and the crystals. Since fluorescence lifetimes are much more sensitive to environmental conditions than the wavelengths of emission maxima, the identical lifetimes convincingly reaffirm the original suggestion based on the spectral measurements that the Ans environment is virtually the same in the crystals and in solution at pH 3.6.

A crystal of Ans-α-CHT, pH 3.6, which had been soaking for about 1 month, was mounted in a capillary and examined X-ray crystallographically. The axial intensity distributions showed significant intensity changes with respect to the native enzyme, suggesting that Ans was binding to the enzyme in the crystal; moreover, the unit cell parameters showed that the volume of the derivative crystal apparently increased slightly (Table I). A three-dimensional set of 2.8-Å resolution intensity data was collected from this crystal. The data were processed and converted to a "best" difference electron density map in a manner similar to that described elsewhere (Tulinsky et al., 1973a; Vandlen & Tulinsky, 1973). The difference map was drawn at a scale of 2 cm Å^{-1} to correspond to a model of α-CHT. The map displayed two prominent saucer-shaped regions of density reaching 0.40 e Å^{-3} in height [$\sim 8\sigma(\Delta\rho)$][1] which could readily be fitted with Kendrew models of Ans. These regions are located in the vicinity of the amino terminus of the A chain of α-CHT (Cys-1–122) and are situated between dimers related by an approximate local "interdimer" twofold rotation axis (dyad B of Figure 2). In fact, from only a cursory inspection, it was not clear whether the binding was intramolecular (e.g., 1 and 1′ or 2 and 2′, Figure 2) or intermolecular (1–2′ and 1′–2). However, $PtCl_4^{2-}$ and PtI_4^{2-} are known to bind intramolecularly in this region near Cys-1–122 (Sigler et al., 1968; Tulinsky et al., 1973a). Since the Ans difference density is within van der Waals contact of the disulfides of the two independent Cys-1–122 residues, it appears that the Ans is also binding intramolecularly. In addition to the ANS density, there were some other smaller regions corresponding to small changes in the structure of α-CHT in the vicinity of the Ans binding. Otherwise, the remainder of the difference map was generally below background level.

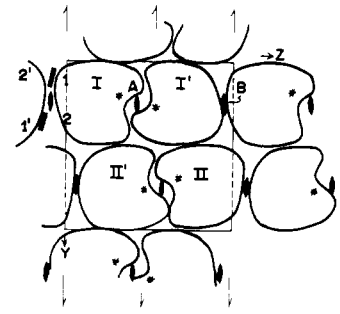

FIGURE 2: Schematic packing diagram of α-CHT viewed down the α* direction. Molecules I and I′ form an asymmetric unit and are related by noncrystallographic twofold axes *A* and *B*; asymmetric units related by crystallographic twofold screw axes are shown appropriately parallel to the *y* axis; asterisks denote active site regions near the center of dimer; 1 and 1′ denote intramolecular Ans binding sites; 2 and 2′ denote close Ans intermolecular contacts.

After the analysis of the structure of the Ans-α-CHT, pH 3.6 complex was essentially completed and the crystals had been soaking for an additional 6 months, the diffraction pattern of the latter was examined prior to changing of the pH of the mother liquor of the crystals. To our surprise, the unit cell dimensions increased significantly (Table I), and the intensities showed additional but small changes beyond those observed previously. A three-dimensional set of 2.8-Å resolution intensity data was collected from one of these crystals. The difference electron density map resulting from the data proved to be very similar to the previous difference map. The peak heights of the Ans substitution remained essentially the same. The principal difference between the two maps was simply a general small increase in the peak heights of difference peaks associated with the structural changes accompanying Ans binding.

Ans-α-CHT at pH 6.6. The pH of the 6-month-soaked crystals of Ans-α-CHT, pH 3.6, was increased several times daily by removal of 0.2-mL aliquots from 3 mL of the storage solution (originally 75% saturated ammonium sulfate and saturated in Ans at pH 3.6) and addition of 0.2-mL aliquots of 75% saturated ammonium sulfate solution saturated in Ans at pH 6.6. After about 1 week, the pH of the mother liquor soaking solution had attained a value of 6.6.

[1] $\sigma(\Delta\rho)$ is the observed root mean square $\Delta\rho$ given by

$$\sigma(\Delta\rho) = \frac{1}{V}\left(\sum_{xyz}[\Delta\rho(xyz)]^2/N\right)^{1/2}$$

where N is the number of points in the summation and V is the volume of the unit cell.

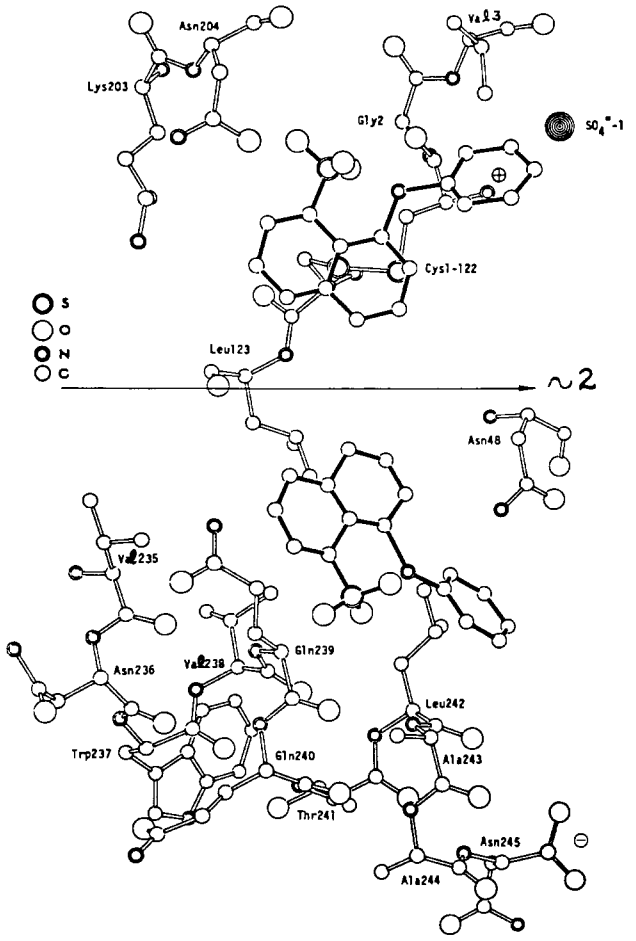

FIGURE 3: Drawing of the vicinity of Ans binding viewed down the c^* direction of crystal. Ans molecules are shaded; the local interdimer twofold axis is shown appropriately; the lower part of the drawing constitutes the remaining environment of upper Ans and vice versa; Ans molecules and the local twofold axis are in a plane perpendicular to view; Ans sulfonate and phenyl rotational orientations are arbitrary but reasonable (see text and footnote 2).

A crystal of Ans–α-CHT, pH 6.6, was then examined X-ray crystallographically. The unit cell volume of the crystals decreased dramatically (Table I). This response to pH change is *different* from that observed with the native enzyme (Mavridis et al., 1974) which shows a slight increase in volume (Table I). In addition, the diffraction pattern of the Ans–α-CHT, pH 6.6 crystals showed changes in intensity with respect to the Ans–α-CHT, pH 3.6 structure. Since the pattern was generally similar to that of the Ans–α-CHT, pH 3.6 derivative, the changes in intensity appeared to be due to changes in the structure of the Ans–α-CHT, pH 3.6 conformer which could also be responsible for the fluorescence decrease and red shift with increase in pH (Johnson et al., 1979). Therefore, a three-dimensional set of 2.8-Å resolution intensity data was collected from this crystal, and it was converted to a best difference electron density map. As expected, the enzyme molecule underwent a number of structural changes similar to those observed by us for the pH 5.4 conformer of native α-CHT (Vandlen & Tulinsky, 1973). However, somewhat less expected was the high degree of similarity in binding of Ans at both pH values.

Results

Ans Binding Site. There are only two general close contacts between the Ans and protein molecules in the crystal, and *they remain the same* following a change in pH from 3.6 to 6.6. The most extensive (nine contacts less than 4.4 Å) and striking of these involves the disulfide bridge of Cys-1–122 (1 or 1′, Figure 2) which is also the amino terminus of the A chain of α-CHT. The other close Ans–protein contact (six contacts less than 4.4 Å) occurs in the vicinity of the side chain of Gln-239′ which is located in a twofold-related neighboring molecule (molecule I′) (2′ or 2, Figure 2). The Gln-239 is part of an α helix formed by residues Val-235–Asn-245 at the carboxyl terminus of the C chain. A drawing of the structure of the environment of Ans in the Ans–α-CHT complex viewed through the Ans toward the Cys-1–122 disulfide bridge is shown above the local twofold axis in Figure 3, while that viewed in the opposite direction, toward the α helix of a neighboring molecule, is shown below the local twofold axis in Figure 3. The Ans molecules and the interdimer local twofold axis are essentially located in a plane perpendicular to the view in Figure 3.

The coordinates of the independent Ans molecules of Ans–α-CHT, pH 3.6, are listed in Table II. Close Ans–protein contacts are listed in Table III, from which the close Cys-1–122 disulfide approach to the naphthyl ring of Ans can be noted, particularly with respect to ring A (Figure 3).

Table II: Coordinates of Bound Ans Molecules[a]

	site 1			site 1′		
atom[b]	x	y	z	x	y	z
1	0.741	0.224	−0.012	0.747	0.363	0.006
2	0.757	0.239	−0.017	0.764	0.348	0.016
3	0.749	0.258	−0.022	0.753	0.331	0.022
4	0.721	0.264	−0.025	0.726	0.326	0.010
5	0.677	0.253	−0.025	0.682	0.339	−0.012
6	0.659	0.238	−0.019	0.668	0.355	−0.027
7	0.667	0.218	−0.016	0.680	0.373	−0.029
8	0.694	0.214	−0.015	0.706	0.377	−0.015
9	0.713	0.229	−0.018	0.721	0.360	−0.007
10	0.702	0.249	−0.021	0.709	0.343	−0.001
1′	0.780	0.199	−0.023	0.787	0.393	0.013
4′	0.834	0.192	−0.027	0.800	0.409	0.006
N	0.751	0.203	−0.015	0.760	0.385	0.000
S	0.707	0.192	−0.014	0.720	0.397	−0.016

[a] Coordinates are fractional referred to the crystallographic axes; origin along y defined is as in Tulinsky et al. (1973a); the local twofold axis is approximately parallel to the a^* axis at $y = 0.291$. [b] Numbering as in structure I, Johnson et al. (1979).

Table III: Close Protein Contacts with Ans[a]

protein atom	Ans	d^b (Å)
Site 1		
Cys-1 – NH_3^+	N	4.2
Cys-1 – S	2	3.0
Cys-1 – C_{γ_2}	1′	4.4
Cys-122 – S	9	2.9
Cys-122 – S	S	3.8
Lys-203 – C_ϵ	6	4.1
Lys-203 – N_ϵ	6	4.0
Asn-204 – C_γ	S	4.4
Asn-204 – O_γ	S	3.5
Site 2′		
Asn-48′ – C_γ	4′	4.4
Leu-123′ – C_δ	10	4.4
Gln-239′ – C_δ	6	3.2
Gln-239′ – C_δ	7	3.1
Leu-242′ – C_γ	1′	4.0
Leu-242′ – C_γ	4′	3.4
Other Important Contacts		
Cys-1 – NH_3^+	S	5.9
SO_4^{2-} – 1	4′	4.9
Cys-1 – NH_3^+ – SO_4^{2-} – 1		3.2

[a] See Figure 2 for exact nature of site designations. [b] Estimated error: ±(0.6–0.7) Å.

Another prominent feature of this environment is the ion pair consisting of the quaternary N-terminal nitrogen atom of Cys-1–122 and its sulfate counterion separated by about 3.2 Å (Table III and Figure 3), the latter having been located previously by a sulfate–selenate exchange experiment (Tulinsky & Wright, 1973). Since Ans is a negative ion at pH 3.6, it is somewhat surprising that the binding of Ans in the same general vicinity did not significantly disturb the ion pair. Interestingly, however, the sulfonate group of Ans fits into an alternating charge array involving Asp-128 – CO_2^-, Lys-203 – NH_3^+, Ans – SO_3^-, Cys-1 – NH_3^+, SO_4^{2-} – 1 (see Figure 3 also). The charge centers are separated by approximately 5.0, 7.5, 5.8, and 3.2 Å, respectively. Although these distances appear to be large for strong interactions, this is due to the fact that hydrogen atoms intervene between the charge centers, limiting approaches. More importantly, the charged array serves to stress the generally polar nature of the Ans binding region 1 and 1′. Other polar features in the binding locale include the side chain of Asn-204 and the side chain of Gln-239′ from another molecule. The only nonpolar side chains in the region are Leu-242′, which makes a minor contact with the phenyl group of Ans, and Val-3 and Ala-206, both of which are relatively small sterically.

From the opposite side, the Ans makes a close contact with the carboxyamide side chain of Gln-239′ and, less importantly, with a methyl group of Leu-123′ and C_γ of Asn-48′, all of a neighboring molecule (below local twofold of Figure 3). Of the six contacts (Table III), only three involve the naphthalene portion of Ans. The Ans here appears to span the planar surface of a hemispherical nonpolar cavity created by the side chains of Ile-47′, Leu 123′, Val-235′, Val-238′, and Leu-242′. These residues are part of a larger internal spherical nonpolar cavity near the center of the molecule (Tulinsky et al., 1973b) between the two cylinders (Birktoft & Blow, 1972) or folding domains of α-CHT. Part of the carboxyl terminal α helix contributes prominently to this region (Figure 3). However, most of these nonpolar features are quite distant to the Ans, especially relative to the proximity of the latter to the disulfide of Cys-1–122. The C_δ atom of the side chain of Gln-239′ is about 3.1 and 3.2 Å, respectively, from C_7 and C_6 of the naphthalene ring of Ans. Finally, all the close contacts in this region are far removed from the more chemically active anilino and sulfonate groups of Ans (6.0–8.0 Å).

The local twofold relationship between the difference densities corresponding to the independent Ans molecules is excellent, in both position and peak height, so that the fit of a model of Ans in each case leads essentially to an identical molecular orientation and conformation (Figure 3). Since the density corresponding to the phenyl group of Ans possessed axial symmetry about the N–$C_{1'}$ direction, it was not possible to assign a rotational conformation and thus determine the coordinates of the $C_{2'}$, $C_{3'}$, $C_{5'}$, and $C_{6'}$ atoms of the ring.[2] However, since a rotation about the C_1–N bond displaces the phenyl ring, it was possible to assign $C_{1'}$ coordinates and to calculate a $C_{1'}$–N–C_1–C_2 torsion angle. A high-resolution X-ray crystallographic structure determination of a monoclinic crystal form of an ammonium salt of Ans has been carried out by us (Weber, 1978) so that parameters of interest characterizing the monoclinic structure can be compared (1) with those of another high-resolution ammonium Ans structure determination (triclinic crystal form) with two molecules of Ans per asymmetric unit (Cody & Hazel, 1977) and (2) with parameters obtained from the Ans–α-CHT complex. The torsional angle and the angle between the planes of the phenyl and napthyl rings of the foregoing are listed in Table IV from which it can be seen that the $C_{1'}$–N–C_1–C_2 torsion angle of Ans in the complex is similar to Ans(1) of Cody & Hazel (1977) but different from Ans_{MSU} and Ans(2). Lastly, the anilino hydrogen and the sulfonate oxygen atoms of Ans are sterically crowded. This precludes classical linear hydrogen bonding although it does not preclude an interaction among these atoms.[3]

Table IV: Comparison of Conformations of Ans

parameter	Ans–α-CHT (deg)	Cody & Hazel (1977) Ans_{MSU}[a] (deg)	Cody & Hazel (1977) Ans-(1) (deg)	Cody & Hazel (1977) Ans-(2) (deg)
$C_{1'}$–N–C_1–C_2[b]	~10	43	22	−46
α[c]	?	61	63	127

[a] Weber (1978). [b] Defined as zero when $C_{1'}$ is coplanar with N, C_1, and C_2. [c] Angle between planes of phenyl and naphthyl rings.

While the changes in protein structure accompanying Ans binding will be discussed in detail below, it can be mentioned that the difference map of Ans–α-CHT, pH 3.6, shows a pronounced density gradient associated with the side chain of Gln-239′. Upon Ans binding, there is a rotation of the side chain of Gln-239′ about the C_γ and C_δ bond such that the polar end of the side chain is removed from the close proximity of the naphthyl ring of Ans. This shift is of the order of 1 Å and may be restrained by a possible interaction of the side chain with that of Lys-203 of another molecule. The side chains of Lys-203 and Lys-203′ also move away from the fluorescence probe but to a lesser degree. Changes in structure on the opposite side of the Ans, near Cys-1–122, are restricted to those apparently involving solvent and do not always show local twofold equivalence. The region leading away from the quaternary terminal nitrogen along the local twofold axis (Figure 3) is generally composed of solvent. From all appearances, the Ans probably approaches the protein binding sites from this direction in the crystal.

Independent Evidence for the Ans Binding Site. Since the Ans binding site lies in an intermolecular region of the crystal, deduction of its intramolecular binding mode was based on the closeness and extent of van der Waals contacts. Although these clearly show that Ans contacts with the protein are more intimate in the Cys-1–122 region, nonetheless, the possibility existed that the binding site in solution may be associated with the more nonpolar α-helical region, even though the van der Waals contacts there were fewer. In order to establish the Ans binding site more definitely, use was made of the fact the $PtCl_4^{2-}$ and PtI_4^{2-} are known to bind near Cys-1–122 in crystals of α-CHT (Sigler et al., 1968; Tulinsky et al., 1973a).

The haloplatinites have been reported to bind strongly at three specific sites in crystals of α-CHT. One of these involves an interaction with the terminal amino group of Cys-1–122 and at least one of the sulfur atoms of the disulfide bridge. The other two sites are in the active site region of the enzyme. Ans has already been shown not to bind at the active site α-CHT (Johnson et al., 1979). Thus, if Ans binds near Cys-1–122 in solution, then PtI_4^{2-} should perturb its fluorescence significantly, whereas the PtI_4^{2-} should be essentially without effect if the Ans were bound near the nonpolar α-helical region of the enzyme 10 Å below the Ans binding site.

[2] The angle between the planes of the phenyl and naphthyl rings in Figure 3 was chosen to optimize the van der Waals contacts within the Ans molecule.

[3] The orientation of the sulfonate in Figure 3 is arbitrary.

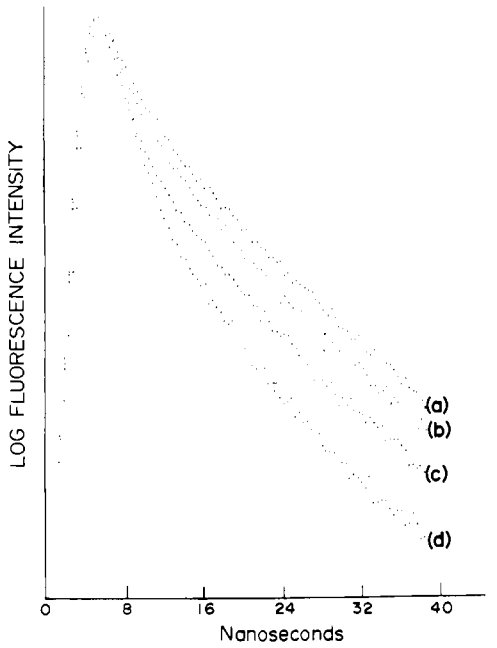

FIGURE 4: Fluorescence decay curves of Ans–α-CHT in the presence of increasing concentrations of K_2PtI_4. (a) $[PtI_4^{2-}] = 0$ M, (b) $[PtI_4^{2-}] = 1.3 \times 10^{-5}$ M, (c) $[PtI_4^{2-}] = 3.8 \times 10^{-5}$ M, (d) $[PtI_4^{2-}] = 1.3 \times 10^{-4}$ M, [α-CHT] = 10^{-4} M, [ANS] = 5×10^{-5} M.

The fluorescence decay curves of Ans–α-CHT in the presence of increasing concentrations of K_2PtI_4 are shown in Figure 4. The effect of PtI_4^{2-} is to appreciably reduce the contribution of the 12-ns component which corresponds to bound Ans fluorescence. This is particularly evident in the presence of 1.3×10^{-4} M PtI_4^{2-} (Figure 4, curve d).

In an effort to approximate conditions in the crystal more closely, the PtI_4^{2-} experiment was also repeated in the presence of 25 and 50% saturated ammonium sulfate, and comparable results were obtained. Similar quenching of tosylated Ans–α-CHT fluorescence by PtI_4^{2-} was also observed.

Quenching of the fluorescence of Ans–α-CHT solutions upon the addtion of small amounts of PtI_4^{2-} can be accounted for in terms of competitive displacement of Ans from its binding site or in terms of PtI_4^{2-} binding near the Ans; the latter possibility is less likely due to steric considerations. Heavy-atom quenching of bound Ans by random collision with PtI_4^{2-}, which causes an enchancement of intersystem crossing at the expense of fluorescence, would require large concentrations of PtI_4^{2-} (10^{-2} M or larger). Moreover, at such concentrations, essentially all of the PtI_4^{2-} would be bound to α-CHT. On the other hand, if Ans binds at the carboxy-terminal site, PtI_4^{2-} could only quench the emission via random collisons, since the latter does not bind at this site.

In an effort to determine the likelihood of collisional quenching, the behavior of a highly fluorescent solution of 5×10^{-5} M Ans in *n*-propyl alcohol was examined upon addition of PtI_4^{2-} ion. The lifetime of Ans fluorescence in *n*-propyl alcohol is about 10.2 ns. The fluorescence decay curve is not appreciably affected by the addition 3.8×10^{-3} M PtI_4^{2-} (i.e., very large concentrations of PtI_4^{2-} are required to produce even a small quenching effect collisionally). To further rule out the possibility of such quenching in Ans–α-CHT, the effect of addition of iodide ion, a very effective heavy-atom quencher of aromatic fluorophores (Burstein, 1968; Lehrer, 1971), was studied. There was no measurable effect on the fluorescence of Ans in α-CHT solutions, even in the presence of 10^{-3} M KI.

From the foregoing, it is clear that PtI_4^{2-} quenching of Ans–α-CHT fluorescence by the collisional mechanism is insignificant and that PtI_4^{2-} either competes for or binds near the Ans binding site. It therefore not only appears that the binding site for Ans is the same in solution and in the crystal but also that the binding site is in the region of the amino terminus of the A chain (Cys-1–122) of the enzyme.

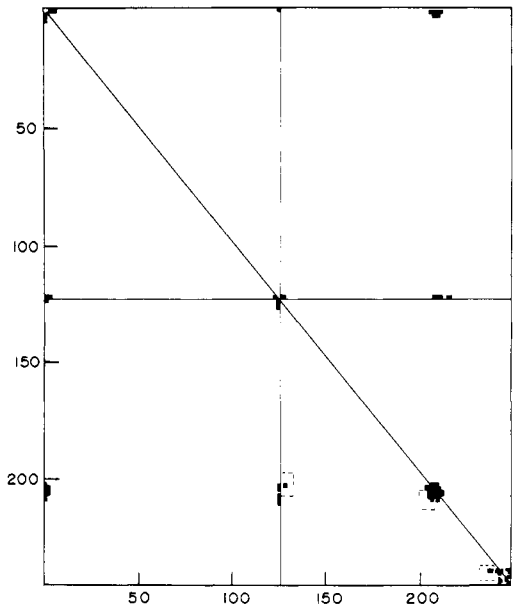

FIGURE 5: Diagonal plot of difference density between Ans–α-CHT, pH 3.6, and α-CHT, pH 3.6. Substitution is blocked at ≤12 Å; nine changes ($|\Delta\rho| > 0.17$ e Å^{-3}) accompanying substitution blocked at ≤9 Å and enclosed by broken lines; interactions with molecule I are below and with molecule I′ are above the diagonal.

Changes in Protein Structure of Ans–α-CHT, pH 3.6. The Ans binding and subsequent perturbation of the protein structure may be conveniently examined by means of a difference diagonal plot (DDP) (Tulinsky et al., 1978; Hibbard & Tulinsky, 1978). This plot is an extension of the well-known α-carbon diagonal distance plot (Nishikawa et al., 1972; Rossman & Liljas, 1974; Kuntz, 1975) and is a way of expressing a difference electron density in a diagonal distance plot format. An $N \times N$ matrix is formed with elements r_{ij} which are given by

$$r_{ij}(k) = |\mathbf{C}_i - \delta_k| + |\mathbf{C}_j - \delta_k|$$

where $\mathbf{C}_i$, $\mathbf{C}_j$, and δ_k are coordinate vectors of the *i*th and *j*th α-carbon atoms of α-CHT and the *k*th peak of the difference density, respectively, and N is the number of amino acid residues of α-CHT. This is then contoured at some convenient distance or distances. Moreover, since $r_{ij} = r_{ji}$, only half of the DDP is unique so that the entire plot may be used to represent the changes occurring in both molecules of α-CHT dimer by plotting the respective interactions above (molecule I′, Figure 5) and below (molecule I, Figure 5) the diagonal. We have found that 9.0 Å was a meaningful lower limit for representing the r_{ij} of protein structural changes attending Ans binding but that a level of 12 Å was better to represent the Ans contacts since the latter binds on the surface of the protein. The DDP corresponding to the contacts made by the Ans substitution at pH 3.6 and the difference peaks accompanying the substitution are shown in Figure 5 where broken lines are used to enclose the latter.[4]

[4] The DDP maps are reproduced from a line printer plot (10 characters per inch, eight lines per inch). This results in a slight distortion and hence a rectangular shape for the DDP. This results in a slight distortion and hence a rectangular shape for the DDP.

In an effort to approximate the shape of the volume of the difference density of the Ans substitution for the DDP calculation, the Ans was represented in terms of eight appropriately spaced points near its perimeter. From Figure 5, it can be seen that the substitution shows excellent local twofold symmetry and clearly reveals the principal Ans–protein interactions (e.g., Cys-1–122, Lys-203 locale, and Gln-239′). Moreover, of the 40 interactions (*ij* blocks) occurring below the diagonal due to the Ans (molecule I), all but nine are generated by the N-terminal binding environment; with molecule I′, the corresponding numbers are 34 and 5. The nine- and five-block features are associated with the α-helical C-terminal region of the enzyme. Thus, it is clear that, in addition to being generally closer, the Ans maintains a more extensive contact with the protein in the disulfide region and that contact with the helical regions is relatively minor and simply represents an intermolecular contact arising from packing of molecules in the crystal.

The Ans difference map contained eight small peaks in the vicinity of binding in addition to the substitution itself. These ranged from 0.17 e $Å^{-3}$ ($\sim 3\sigma$) to 0.25 e $Å^{-3}$, and their effect on the DDP calculation was to give rise to those features enclosed by broken lines in Figure 5. These features occur exclusively in cylinder 2 (Birktoft & Blow, 1972) or the B folding domain (sequence > 122) of α-CHT (Tulinsky et al., 1978). Moreover, since they are close to the diagonal of the DDP, they are necessarily localized near these particular main-chain positions. As can be seen in Figure 5, only three regions are involved (near Pro-124, Lys-203, Lys-203–Asn-204, and Gln-239), and all are located in the vicinity of the Ans binding site. Other difference peaks in the binding region, but on the border line of significance, suggest small changes in the location of solvent molecules, some changes being symmetric and some not. Otherwise, no signficant changes appear elsewhere in the protein.

Changes in the Ans Binding Site at pH 6.6. The difference density corresponding to Ans in the Ans–α-CHT, pH 6.6, map is nearly identical with that observed at pH 3.6, and only a few small changes were observed in the binding environment upon comparison of difference Fourier syntheses of Ans–α-CHT, pH 3.6, with α-CHT, pH 3.6, and Ans–α-CHT, pH 6.6, with α-CHT, pH 3.6. The previously discussed Gln-239 difference gradient underwent a diminution at pH 6.6. There were also some smaller changes involving the Lys-203 peaks. In summary, only very small alterations in or related to the Ans binding site region which accompany a change in pH from 3.6 to 6.6 have been observed which are unique to the protein–probe complex.

Comments of the DDP. Features in the ΔpH DDP may also be used to indicate some of the limitations of the technique as presently constituted. Specifically, the alterations in protein structure which accompany the pH change are, in the majority, surface changes, changes involving amino acid side chains, and changes located in the dimer interface (Vandlen & Tulinsky, 1973). The DDP calculation is currently restricted to the consideration of α-carbon difference peak contacts, thus limiting its use for summarizing side-chain movements. This is especially so on the surface of the protein where there are necessarily less contacts.[5] Furthermore, the calculation does not include r_{ij} between the different monomers in the dimer interface region. Therefore, a number of changes, which have been characterized by detailed analysis of the pH 5.4 conformer of α-CHT, are underrepresented in the DDP.

Conversely, the DDP accurately represents any lack of major perturbation in tertiary structure, and the involvement of certain amino acids in regions of important change. In the latter category, one observes features in the Tyr-146, and Try-146′, Ala-149, Asp-64, and Phe-39 regions which have been described and discussed in detail previously (Vandlen & Tulinsky, 1973). A difference peak generating interactions in the Ser-217–Ser-218 region also generates a block at Ser-217′–Ser-218′, demonstrating a close contact between monomer polypeptide chains (Tulinsky et al., 1973b). Along similar lines, the DDP calculation between pH conformers (5.4–3.6) contains a total of 51 blocks, of which 47 have a multiplicity (Hibbard & Tulinsky, 1978) of one, two have a multiplicity of two, and two have a multiplicity of three. All of the higher multiplicity interactions involve Tyr-146 and Tyr-146′, indicating the sensitivity of this carboxylic B-chain terminus to pH change in both monomers.

Discussion

The most striking feature of the structure of the Ans–α-CHT complex is the close contact of the naphthyl ring of Ans to the disulfide bond of Cys-1–122. A recent survey of X-ray crystallographic structures of proteins has revealed the regions of eight globular proteins which show spatial arrangements of alternating sulfur atoms and aromatic groups (Morgan et al., 1978) and which suggest that electron flow might be facilitated through these S–π "chains". Although disulfides are known to quench tryptophan fluorescence in proteins and have been shown to quench indole emission in solution by collision (Cowgill, 1970), nonetheless, Ans fluoresces intensely at low pH. The quenching of tyrosine and tryptophan by model disulfide compounds has been shown to involve an excited or intermolecular charge-transfer state from the fluorophore to the sulfur atoms (Arian et al., 1970; Bent & Hayon, 1975). The apparent anomaly in the case of the Ans–α-CHT complex could be accounted for in terms of an unfavorable orientation of the disulfide group in relation to the naphthyl ring and the lack of enough rotational freedom of the former to reorient more favorably for quenching during the lifetime of the excited state of Ans. Another possibility is that fluorescence quenching via a charge-transfer mechanism involving a disulfide requires a mobile polar medium to stabilize the charge separation.

More recent work from our laboratory, which has produced a 1.8-Å resolution electron density map of α-CHT, pH 3.6 (Raghavan & Tulinsky, 1979), has given us some further insights concerning the enhanced fluorescence of Ans bound to α-CHT. An examination of the map in the vicinity of the Ans binding suggests that ordered solvent molecules are present in the region. Since the fluorescence decay curves of Ans–α-CHT in solution and in the crystal at pH 3.6 are the same, the immediate molecular environments of the Ans in the two cases must also be very similar: the Ans is on the surface in a generally polar region near an array of charged amino acid residues, it interacts strongly with a disulfide group, and it is accessible to polar solvent molecules which, in addition, appear to be ordered. The accessibility has been amply demonstrated by accessibility of the site to Ans itself and by the effectiveness of PtI_4^{2-} quenching. The enhanced fluorescence of bound Ans therefore might be due to a local high microviscosity in the protein complex which produces a long relaxation time on the fluorescence time scale for protein and solvent dipoles in the vicinity of Ans.

The pH dependence of fluorescence in the Ans–α-CHT complex is dramatic in solution but not in the crystal. The

[5] Since solvent does not enter into consideration, its volume is excluded from the calculation, thus generally giving rise to fewer r_{ij} satisfying the 9.0-Å limit in this region.

fluorescence decay curves of Ans–α-CHT crystals at pH 6.9 and 3.6 measured at 490 nm are very similar and show a lifetime at high pH which is only slightly less than that at pH 3.6. This is in contrast to the solution results where the fluorescence decay curves are drastically altered with an increase in pH (Johnson et al., 1979). In the preceding communication, we have suggested that a change in the degree of mobility of water molecules near the Ans binding site due to protein conformational changes induced by increasing pH could explain the dramatic pH effect on fluorescence intensity. Such conformational changes could conceivably be severely limited in the crystal.

In summary, the foregoing results show that fluorescence enhancements that occur upon the binding of fluorescence probes such as Ans to proteins may not always result from a hydrophobic site on the protein as has been commonly thought heretofore and suggest the need for caution in the interpretation of fluorescent changes as such probes interact with macromolecules.

In a previous communication of this series (Tulinsky et al., 1978), it was noted that a single nonactive site substitution of *N*-formyltryptophan (form-Trp) is found in crystals of α-CHT at pH 3.6. This secondary site is intramolecular and borders that of the Ans site. At one extremity, to which the six-membered portion of the indole ring was assigned, the difference electron density of form-Trp is in contact with dyad B and shows no local twofold symmetry. The form-Trp substitution is more interior to monomer I than that of Ans and only binds in environment 1 (Figure 2). From the perspective of Figure 3, the form-Trp is located to the left of the Ans, at a depth placing it between the disulfide and δ carbon of Lys-203. The nonindole portion appears to be in the same general vicinity as the sulfonyl group of Ans. The relative peak heights of the difference electron density of Ans (0.40 e $Å^{-3}$) and form-Trp (0.23 e $Å^{-3}$) suggest that the latter has a lower affinity for this binding site than has Ans.

Acknowledgments

We thank Dr. D. J. Duchamp, The Upjohn Co., Kalamazoo, MI, for the use of a computer graphics facility and D. Carr for technical assistance in some of the fluorescence decay studies.

References

Arian, S., Benjamini, M., Feitelson, J., & Stein, G. (1970) *Photochem. Photobiol. 12*, 481.

Bent, D. V., & Hayon, E. J. (1975) *J. Am. Chem. Soc. 97*, 2612.

Birktoft, J. J., & Blow, D. M. (1972) *J. Mol. Biol. 68*, 187.

Brand, L., & Gohlke, J. R. (1972) *Annu. Rev. Biochem. 41*, 843.

Burstein, E. A. (1968) *Biofizika 13*, 433.

Cody, V., & Hazel, J. (1977) *J. Med. Chem. 20*, 12.

Cowgill, R. W. (1970) *Biochim. Biophys. Acta 207*, 556.

DeToma, R. P., Easter, J. H., & Brand, L. (1976) *J. Am. Chem. Soc. 98*, 5001.

Edelman, G. M., & McClure, W. O. (1968) *Acc. Chem. Res. 1*, 65.

Einarsson, R., Eklund, H., Zeppzauer, E., Boiew, T., & Branden, C. (1974) *Eur. J. Biochem. 49*, 41.

Hibbard, L. S., & Tulinsky, A. (1978) *Biochemistry 17*, 5460.

Johnson, J. D. (1978) Ph.D. Thesis, Michigan State University.

Johnson, J. D., El-Bayoumi, M. A., Weber, L. D., & Tulinsky, A. (1979) *Biochemistry* (preceding paper in this issue).

Kosower, E. M., Dodiuk, H., Tanizawa, K., Ottolenghi, M., & Orbach, N. (1975) *J. Am. Chem. Soc. 97*, 2167.

Kuntz, I. D. (1975) *J. Am. Chem. Soc. 97*, 4362.

Lehrer, S. S. (1971) *Biochemistry 10*, 3254.

Mavridis, A., Tulinsky, A., & Liebman, M. N. (1974) *Biochemistry 13*, 3661.

Morgan, R. S., Tatsch, C. E., Gushard, R. H., McAdon, J. M., & Warme, P. K. (1978) *Int. J. Pept. Protein Res. 11*, 209.

Nishikawa, K., Ooi, T., Isagai, Y., & Saito, N. (1972) *J. Phys. Soc. Jpn. 32*, 1331.

Penzer, G. R. (1972) *Eur. J. Biochem. 25*, 218.

Raghaven, N. V., & Tulinsky, A. (1979) *Acta Crystallogr.* (in press).

Rossmann, M. G., & Liljas, A. (1974) *J. Mol. Biol. 85*, 177.

Sigler, P. B., Blow, D. M., Matthews, B. W., & Henderson, R. (1968) *J. Mol. Biol. 35*, 143.

Tulinsky, A., & Wright, L. H. (1973) *J. Mol. Biol. 81*, 47.

Tulinsky, A., Mani, N. V., Morimoto, C. N., & Vandlen, R. L. (1973a) *Acta Crystallogr., Sect. B 29*, 1309.

Tulinsky, A., Vandlen, R. L., Morimoto, C. N., Mani, N. V., & Wright, L. H. (1973b) *Biochemistry 12*, 4185.

Tulinsky, A., Mavridis, I. M., & Mann, R. F. (1978) *J. Biol. Chem. 253*, 1074.

Vandlen, R. L., & Tulinsky, A. (1973) *Biochemistry 12*, 4193.

Weber, L. D. (1978) Ph.D. Thesis, Michigan State University.